

Published in final edited form as:

Neuropharmacology. 2011 ; 60(2-3): 405–409. doi:10.1016/j.neuropharm.2010.10.010.

Temporary inhibition of AMPA receptors induces a prolonged improvement of motor performance in a mouse model of juvenile Batten disease

Attila D. Kovács^{1,2,6}, Angelika Saje⁴, Andrew Wong⁴, Gábor Szénási⁵, Péter Kiricsi⁵, Éva Szabó⁵, Jonathan D. Cooper⁴, and David A. Pearce^{1,2,3,6,7}

¹Center for Neural Development and Disease, University of Rochester School of Medicine and Dentistry, Rochester, NY, 14642, USA

²Department of Biochemistry and Biophysics, University of Rochester School of Medicine and Dentistry, Rochester, NY, 14642, USA

³Department of Neurology, University of Rochester School of Medicine and Dentistry, Rochester, NY, 14642, USA

⁴Pediatric Storage Disorders Laboratory, Department of Neuroscience, Centre for the Cellular Basis of Behaviour, MRC Centre for Neurodegeneration, James Black Centre, King's College London, Institute of Psychiatry, London SE5 9NU, UK

⁵Division of Preclinical Research, EGIS Pharmaceuticals Plc., Budapest, Hungary

⁷Department of Pediatrics, Sanford School of Medicine, University of South Dakota, Sioux Falls, South Dakota, 57104 USA

Abstract

Mutations in the *CLN3* gene cause juvenile Batten disease, a fatal pediatric neurodegenerative disorder. The *Cln3*-loss-of-function (*Cln3^{Δex1-6}*) mouse model of the disease displays many pathological characteristics of the human disorder including a deficit in motor coordination. We have previously found that attenuation of α -amino-3-hydroxy-5-methyl-4-isoxazolepropionate (AMPA)-type glutamate receptor activity in one-month-old *Cln3^{Δex1-6}* mice resulted in an immediate improvement of their motor skills. Here we show that at a later stage of the disease, in 6-7-month-old *Cln3^{Δex1-6}* mice, acute inhibition of AMPA receptors by a single intraperitoneal injection (1 mg/kg) of the non-competitive AMPA antagonist, EGIS-8332, does not have an immediate effect. Instead, it induces a delayed but prolonged improvement of motor skills. Four days after the injection of the AMPA antagonist, *Cln3^{Δex1-6}* mice reached the same motor skill level as their wild type (WT) counterparts, an improvement that persisted for an additional four days. EGIS-8332 was rapidly eliminated from the brain as measured by HPLC-MS/MS. Histological analysis performed 8 days after the drug administration revealed that EGIS-8332 did

© 2010 Elsevier Ltd. All rights reserved.

Corresponding author: David A. Pearce, PhD Sanford Children's Health Research Center 2301 E. 60th Street, Sioux Falls, South Dakota, 57014, Tel: (605)312-6004, Fax: (605)328-0401 PearceD@SanfordHealth.org.

⁶Current affiliation: Sanford Children's Health Research Center, Sanford Research/USD

Publisher's Disclaimer: This is a PDF file of an unedited manuscript that has been accepted for publication. As a service to our customers we are providing this early version of the manuscript. The manuscript will undergo copyediting, typesetting, and review of the resulting proof before it is published in its final citable form. Please note that during the production process errors may be discovered which could affect the content, and all legal disclaimers that apply to the journal pertain.

Conflict of interest

None of the authors of this paper has any conflict of interest relating to the publication.

not have any impact upon glial activation or the survival of vulnerable neuron populations in 7-month-old *Cln3^{Δex1-6}* mice.

We propose that temporary inhibition of AMPA receptors can induce a prolonged correction of the pre-existing abnormal glutamatergic neurotransmission in vivo for juvenile Batten disease.

Keywords

neuronal ceroid lipofuscinoses; *Cln3*; AMPA receptor; EGIS-8332; rotarod

1. Introduction

Batten disease (also known as Neuronal Ceroid Lipofuscinoses), is a group of recessively inherited, fatal lysosomal storage disorders characterized by progressive neurodegeneration (Cooper, 2003). Batten disease is the most common degenerative brain disease in children, with an incidence as high as one in 12,500 live births, and with about 440,000 carriers in the USA (Cooper, 2003; Goebel, 1995; Rider and Rider, 1997). Traditionally, different subtypes of Batten disease were categorized based on the onset and clinical course of the disease, but the different forms of the disease are now classified according to the genetic defect that is present.

The juvenile onset form of Batten disease (JNCL) results from mutations in the *CLN3* gene (Consortium, 1995). *CLN3* encodes a lysosomal membrane protein of unknown function (Phillips et al., 2005) and accordingly, the mechanism of how *CLN3* mutations lead to selective neurodegeneration remains elusive. The disease begins between five and eight years of age, with typical clinical symptoms being progressive vision loss, frequent occurrence of seizures, loss of motor skills and progressive cognitive decline, cumulatively leading to premature death in the late teens or early 20s (Goebel and Wisniewski, 2004). No specific treatment is currently available that could halt or slow the progression of the disease.

The *Cln3*-knockout (*Cln3^{Δex1-6}*) mouse model of JNCL exhibits many characteristic features of the human disorder, including a deficit in cerebellar motor coordination (Kovacs et al., 2006; Mitchison et al., 1999; Weimer et al., 2009). Exploring the possible cause(s) of the functional impairment of the *Cln3^{Δex1-6}* cerebellum, we have found that cerebellar granule cells from *Cln3^{Δex1-6}* mice in dissociated cultures and in organotypic cerebellar slice cultures are significantly more sensitive to AMPA-type, but not NMDA-type, glutamate receptor-mediated toxicity than their wild type counterparts (Kovacs et al., 2006), indicating an abnormally enhanced AMPA receptor activity. Attenuating this AMPA receptor activity via a specific AMPA antagonist in one-month-old *Cln3^{Δex1-6}* mice resulted in an immediate improvement of their motor skills (Kovacs and Pearce, 2008), confirming that an abnormally increased AMPA receptor activity contributes to the motor coordination deficit at this early stage of the disease.

The cellular and molecular mechanisms giving rise to the disease symptoms can significantly change during disease progression, as was recently demonstrated in a mouse model of Huntington's disease, another progressive neurodegenerative disorder (Graham et al., 2009). Therefore, we tested if acute inhibition of AMPA receptors is also beneficial at a later stage of JNCL, in 6-7-month-old *Cln3^{Δex1-6}* mice. In these older mice, acute inhibition of AMPA receptors by a single intraperitoneal injection (1 mg/kg) of the non-competitive AMPA antagonist, EGIS-8332 (Gigler et al., 2007; Gressens et al., 2005; Matucz et al., 2004), did not have an immediate effect. Instead, it induced a delayed but prolonged improvement of motor skills. EGIS-8332 was rapidly eliminated from the brain and did not

affect the previously described selective neuronal loss and glial activation (Pontikis et al., 2004; Weimer et al., 2006; Weimer et al., 2009) in 7-month-old *Cln3^{Δex1-6}* mice.

2. Materials and methods

2.1. Animals

In this study 6-7-month-old 129S6/SvEv wild type (WT) and homozygous *Cln3*-knockout (*Cln3^{Δex1-6}*) mice (Mitchison et al., 1999) inbred on a 129S6/SvEv background were used. All mice used in the study were female. Mice were genotyped as described by Mitchison et al. (1999). All procedures were carried out according to the guidelines of the Animal Welfare Act, NIH policies and the University of Rochester Animal Care and Use Committee.

2.2. Rotarod test

An accelerating rotarod (AccuScan Instruments, Inc., Columbus, OH) was used to measure the motor skills of mice. The rotarod measures the ability of the mouse to maintain balance on a motor-driven, rotating rod. Thus, the fore- and hind limb motor coordination and balance can be analyzed (Karl et al., 2003). Due to the repeated, multiple test trials used in our rotarod protocol, motor learning also contributes to the rotarod performance of mice. During the training period, mice were placed on the rotarod starting at zero rpm and accelerating to 24 rpm in 240 seconds. Mice were trained for three consecutive runs. Following training, mice rested for 1 h and then were tested for three Pre-treatment test trials each consisting of three consecutive runs, with 15 min of rest between the trials. Two hours and thirty minutes after the end of the Pre-treatment test, mice were intraperitoneally injected with the noncompetitive AMPA receptor antagonist, EGIS-8332 (synthesized by EGIS Pharmaceuticals Plc, Budapest, Hungary) at a dose of 1 mg/kg (injection volume: 10 ml/kg). Control mice were injected with the vehicle of the drug (20 mM HCl containing 10% DMSO). Thirty minutes, 1, 4, 6 and 8 days after the injection, mice were tested for three test trials each consisting of three consecutive runs, with 15 min of rest between the trials. The latencies to fall from the rotating rod during the testing periods were calculated for each mouse. Fifteen vehicle-injected and fifteen EGIS-8332-treated *Cln3^{Δex1-6}* mice were tested on the rotarod. Thirteen vehicle-injected and twelve EGIS-8332-treated WT mice were also tested on the rotarod.

2.3. HPLC-MS/MS analysis of EGIS-8322 levels in the plasma and brain tissue

EGIS-8332 levels were measured in the plasma and brain of 7-month-old female *Cln3^{Δex1-6}* mice at different time points after a single i.p. injection of the drug (1 mg/kg); n=4 mice at each time point. Blood was taken from the vena cava under isoflurane anaesthesia, and centrifuged for 10 min at 1625 g. After decapitation the brain was removed and weighed. The plasma and brain tissue were stored at -70°C until analysis. Upon thawing the brain tissue was homogenized in a potter. Calibration curves were prepared by adding variable amounts of EGIS-8332 into drug-free plasma and brain homogenate. Both the plasma and homogenized brain tissue were extracted by mixing in a vortex for 30 min using acetonitrile:distilled water (3:1 by volume). Upon centrifuging the supernatants were dissolved in mobile phase A. The HPLC-MS/MS system consisted of a Waters Alliance 2795 HPLC, and a Quattro Ultima Platinum mass spectrometer. Gradient chromatographic separation of EGIS-8332 was achieved with 10 mM ammonium formate, 5% acetonitrile, 0.1% trifluoroacetic acid in distilled water (mobile phase A) and acetonitrile and 0.1% trifluoroacetic acid (mobile phase B) on a Purospher STAR RP-18 column (55-4, 3 μm particle size). A linear gradient from 100% A to 100% B was programmed between 0 and 3 min. Retention window of EGIS-8332 was 0–4 min, detected by a Waters 2487 UV detector. Ionization was performed in the positive ion mode. The dwell time was set to 200 ms, and

the drug was monitored in the multiple-reaction monitoring (MRM) mode. The most abundant fragmentation paths, m/z 363→294 and 363→321 were set for detection of EGIS-8332. The orifice and ring potentials were optimized to the highest signal for the analyte.

2.4. Histological processing

Eight days after vehicle or EGIS-8332 administration, 7-month-old *Cln3^{Δex1-6}* mice were perfusion-fixed with 4% paraformaldehyde (in Dulbecco's phosphate-buffered saline (DPBS), pH 7.4). Seven-month-old untreated wild type (WT) mice were also perfusion-fixed. The brains were post-fixed for 2 h at room temperature and cryoprotected at 4°C in a solution of 30% sucrose in DPBS containing 0.05% sodium azide. Brains were bisected along the midline, and 40µm coronal sections were cut from the left hemisphere on a microtome (Leitz 1321 freezing microtome) and stored in 96 well plates that contained a cryoprotectant solution (30% ethylene glycol, 15% sucrose and 0.05% sodium azide in Tris buffered saline (TBS: 50 mM Tris, 150 mM NaCl, pH 7.6)).

2.5. Nissl staining and stereological estimation of neuron number

To visualize neuronal cytoarchitecture every sixth section of each brain (n= 4, untreated WT mice and vehicle and EGIS-8332 injected *Cln3^{Δex1-6}* mice) was mounted on gelatine/chrome alum-coated Superfrost microscope slides (VWR, Poole, UK), air dried overnight and stained for 30min at 60°C with cresyl fast violet solution (0.05% solution with 0.5 ml of 10% acetic acid per 100 ml of solution were mixed and preheated to 56°C directly before use). Slides were next rinsed in distilled water and differentiated through a graded series of IMS. Finally sections were cleared in xylene and coverslipped with DPX (VWR) (Pontikis et al., 2004).

To survey the survival of neuron populations that are vulnerable in *Cln3^{Δex1-6}* mice, counts were made of the large projection neurons in the thalamus (dorsal lateral geniculate nucleus) and in the medial deep cerebellar nucleus. These counts were obtained using StereoInvestigator software (Microbright Field, Williston, VT) as previously described (Bible et al., 2004). The boundaries of nuclei were defined by reference to landmarks in a mouse brain atlas (Paxinos and Franklin, 2001). The mean coefficient of error (CE) for all individual optical fractionator and nucleator estimates was calculated according to the method of Gundersen (Gundersen and Jensen, 1987) and was less than 0.09 in all these analyses. Images for neuronal cell counts were taken with a 100X oil objective on a Zeiss Axioskop2 MOT microscope (Carl Zeiss Ltd, Welwyn, Garden City, UK), as described previously (Weimer et al., 2009).

2.6. Quantification of GFAP and F4/80 immunoreactivity

To assess the degree of astrocytic and microglial activation every sixth section of each brain (n= 4, untreated WT mice and vehicle and EGIS-8332 injected *Cln3^{Δex1-6}* mice) was immunohistochemically stained for the astrocytic marker glial fibrillary acidic protein (GFAP) and the microglia marker F4/80 as described previously (Weimer et al., 2009). Briefly, sections were first treated with 1% H₂O₂ in Tris-buffered saline (TBS: 50mM Tris, pH 7.6) for 30 min to block endogenous peroxidase activity and subsequently rinsed three times for 5 min in TBS. To minimise non-specific protein binding the sections were incubated with 15% normal serum (serum from the host species of the secondary antibody) in TBS-T (TBS containing 0.3% w/v Triton X-100) for 30 min. Sections were then labelled overnight at 4°C with either a rabbit anti-GFAP (Dako, 1:5000) or a rat anti-F4/80 (Serotec, 1:100) antibody diluted in TBS-T containing 10% normal serum (normal swine serum for GFAP, normal rabbit serum for F4/80). After washing in TBS (3 times, 5 min each), sections were incubated for 2 hours at room temperature with the appropriate biotinylated

secondary antibody (for GFAP: swine anti-rabbit, 1:1000, Vector Laboratories; for F4/80: rabbit anti-rat, 1:200, Vector Laboratories) diluted in TBS-T containing 10% normal serum. After washing in TBS (3 times, 5 min each), sections were incubated for 2 h at room temperature in ABC reagent (avidin-biotinylated enzyme complex) diluted 1:1000 in TBS (Vectastatin Elite ABC kit, Vector Laboratories). After washing in TBS 3 times (5 min each), a standard diaminobenzidine reaction was used to visualize immunoreactivity. Afterwards sections were mounted on Superfrost microscope slides, air dried overnight, cleared in xylene and coverslipped with DPX (VWR).

All photomicrographs were taken with Zeiss AxioCam HR digital camera and Axiovision 4.6 software (Carl Zeiss UK Ltd, Welwyn Garden City, UK). All following analyses were performed with no previous knowledge of treatment. Assessment of GFAP and F4/80 staining was done with a semi-automated thresholding image analysis (Bible et al., 2004; Pontikis et al., 2004). Accordingly, forty non-overlapping pictures from the region of interest were captured from four sequential stained sections. Images were captured under constant conditions (lamp intensity, video camera set up and calibration). Thresholding analysis was then performed using Image Pro Plus image analysis software (Media Cybernetics, Chicago, IL). An appropriate threshold was determined to discriminate specific immunoreactivity from background staining, and was applied subsequently for all analysis.

2.7. Statistical analysis

All rotarod data sets passed the normality test (alpha level 0.05), and therefore, repeated measures one-way and two-way ANOVAs with Bonferroni's test for pairwise multiple comparison were applied in the statistical analysis using GraphPad Prism 4. Repeated measures two-way ANOVA was applied to compare Control and EGIS-8332-treated *Cln3^{Δex1-6}* (Fig. 1) mice as well as Control WT and *Cln3^{Δex1-6}* mice (Fig. 2). Repeated measures one-way ANOVA was used to compare the motor performances between two consecutive time points. Histological data were analyzed by one-way ANOVA with Bonferroni's post-test.

3. Results

3.1. Acute treatment with the AMPA receptor antagonist, EGIS-8332, induces a delayed but prolonged improvement of motor skills in 6-7-month-old *Cln3^{Δex1-6}* mice

In 6-7-month-old *Cln3^{Δex1-6}* mice, EGIS-8332 (1 mg/kg i.p.) did not improve the motor skills 30 min or 1 day after the treatment (Fig. 1A). However, 1 mg/kg EGIS-8332 did provide a significant and prolonged improvement in rotarod performance in *Cln3^{Δex1-6}* mice several days after its injection (Fig. 1A), but had no effect upon the motor skills of age-matched WT mice (Fig. 1B). As expected, WT mice effectively learned during the repeated rotarod tests and were able to improve their motor skills in each test trial. In contrast, vehicle-injected *Cln3^{Δex1-6}* mice had displayed a limited ability to improve their motor skills during the repeated rotarod tests (Fig. 1C) EGIS-8332-treated *Cln3^{Δex1-6}* mice reached the same motor skill level as their wild type (WT) counterparts four days after the drug injection, and remained at the WT skill level even four days later (Fig. 1D).

3.2. EGIS-8332 is eliminated from the brain of *Cln3^{Δex1-6}* mice within 8 h

To examine if EGIS-8332 is quickly eliminated from the brain, the levels of EGIS-8332 were measured by HPLC-MS/MS in the plasma and brain of 7-month-old *Cln3^{Δex1-6}* mice at different time points after the drug injection. As Table 1 shows EGIS-8332 rapidly reached its peak concentration in both brain and plasma and was practically eliminated from the brain 8 h after its administration.

3.3. Acute treatment with EGIS-8332 has no effect on the previously described neuropathological changes in 7-month-old *Cln3^{Δex1-6}* mice

Optical fractionator counts of neuron number revealed that EGIS-8332, as examined 8 days after its injection, had no protective effect on the previously described loss of large projection neurons either in the dorsal lateral geniculate nucleus (LGNd) of the thalamus or in the medial deep cerebellar nucleus (DCN) in 7-month-old *Cln3^{Δex1-6}* mice (Fig. 2A). Similarly, the levels of astrogliosis and microglial activation in the cortex and the cerebellum of *Cln3^{Δex1-6}* mice were also unaffected by EGIS-8332 (Fig. 2B and C; data are not shown for astrogliosis and microgliosis in the cerebellum).

4. Discussion

This study provides evidence that temporary inhibition of AMPA receptors by a single i.p. administration of the non-competitive AMPA antagonist, EGIS-8332, induces beneficial neuroadaptive changes in the *Cln3^{Δex1-6}* mouse model of the incurable juvenile Batten disease. In 6-7-month-old *Cln3^{Δex1-6}* mice representing the midstage of the disease, EGIS-8332 induced a delayed but prolonged improvement of motor skills. Four days after the injection of the AMPA antagonist, *Cln3^{Δex1-6}* mice reached the same motor skill level as their WT counterparts and stayed at the WT skill level for at least four further days. Since EGIS-8332, similarly to other AMPA receptor antagonists, has a relatively short biological half-life in animals [see Table 1 and (Gigler et al., 2007)], it is not likely that the drug can provide effective AMPA receptor antagonism for several days. A more likely assumption is that a temporal inhibition of AMPA receptors in the *Cln3^{Δex1-6}* brain initiates beneficial changes in glutamatergic neurotransmission and synaptic plasticity resulting in a prolonged improvement of motor performance. Recent reports showing that a single administration of the N-methyl-D-aspartate (NMDA) receptor blocker, MK-801 (5 mg/kg), in rats induces long-lasting (4 weeks) changes in synaptic plasticity (Manahan-Vaughan et al., 2008; Wohrl et al., 2007), support this notion.

The next step will be to evaluate how long the improvement in motor performance resulting from acute inhibition of AMPA receptors in *Cln3^{Δex1-6}* mice lasts. Our pharmacological data support the hypothesis that AMPA receptor hyperfunction largely contributes to the neurological deficit in CLN3-deficient mice. This hypothesis was based on our previous results demonstrating that *Cln3^{Δex1-6}* cerebellar granule cells in dissociated cultures and in organotypic cerebellar slice cultures have selectively increased sensitivity to AMPA receptor overactivation (Kovács et al., 2006). Metabolomic profiling via NMR spectroscopy found increased glutamate levels in cerebellar and cerebral extracts of 1-, 2-, 3- and 6-month-old *Cln3^{Δex1-6}* mice by (Pears et al., 2005), and these results also suggest that CLN3-deficiency causes dysregulation of glutamatergic neurotransmission. The abnormal AMPA receptor-mediated neurotransmission, that impairs neurological functions of *Cln3^{Δex1-6}* mice as early as postnatal day 30 (Kovács and Pearce, 2008) and persists at least until the age of 6–7 months (see Fig. 1), is obviously not neurotoxic since with the exception of the neuron loss that is restricted to the LGNd of the thalamus (Weimer et al., 2006) and in the medial deep cerebellar nucleus (Weimer et al., 2009), overt neurodegeneration cannot be detected in the brain of *Cln3^{Δex1-6}* mice until 12 months of age (Pontikis et al., 2004). Although EGIS-8332 treatment didn't afford any protection to either LGNd or DCN neurons, it will be important to determine whether administration of AMPA receptor antagonists can prevent the later onset neuron loss that occurs in *Cln3^{Δex1-6}* mice beyond one year of age.

Activation of glial cells in general is a common event in neurodegenerative diseases (Danton and Dietrich, 2003; Farfara et al., 2008; Venneti et al., 2009), and several previous studies have shown that glial activation also occurs in Batten disease. However, unlike many other neurodegenerative disorders, this activation of glial cells occurs before neuron loss (Bible et

al., 2004; Kielar et al., 2007; Pontikis et al., 2004). It was recently discovered that prolonged inhibition of AMPA receptors prevents neuroinflammation including astrocytic activation (Greene et al., 2008). Acute attenuation of AMPA receptor activity with EGIS-8332 in our study, however, had no effect on astrocytic or microglial activation, probably due to the low-level and short-term inhibition of AMPA receptors on glial cells. These results also suggest that glial activation in *Cln3^{Δex1-6}* mice does not directly contribute to their neurological deficits since EGIS-8332 restored motor coordination to the WT level without impacting gliosis.

The prolonged beneficial effect of an acute treatment with an AMPA receptor antagonist in 6-7-month-old *Cln3^{Δex1-6}* mice (Fig. 1) indicates that administration of low doses of AMPA receptor antagonists that attenuate AMPA receptor function, but avoid a complete and toxic blockade of the receptor is a promising therapeutic approach for juvenile Batten disease, and suggests that this new therapeutic approach will be applicable even at later stages of the disease. The importance of testing such novel therapeutic approaches at different stages of disease progression is highlighted by a recent study in the YAC128 mouse model of the neurodegenerative disorder, Huntington's disease (Graham et al., 2009). Excitotoxicity has been postulated to play a key role in the selective vulnerability of striatal neurons in Huntington's disease. However, these authors showed that while 1.5-month-old YAC128 mice displayed enhanced striatal sensitivity to NMDA receptor-mediated toxicity *in vivo* prior to obvious phenotypic changes, 10-month-old symptomatic YAC128 mice were resistant to NMDA receptor overactivation (Graham et al., 2009).

Our finding that temporary inhibition of AMPA receptors can induce a prolonged correction of the pre-existing abnormal glutamatergic neurotransmission *in vivo* may have important therapeutical implications for other neurodegenerative diseases (Huntington's disease and Parkinson's disease) and neurological disorders (drug addiction and neuropathic pain) where abnormally enhanced glutamatergic neurotransmission plays a pathophysiological role (Bleakman et al., 2006; Chase et al., 2003; Engblom et al., 2008; Fan and Raymond, 2007; Lane et al., 2008). Besides trying to continuously block glutamate receptor activity by chronic treatments in these disorders, the possible longer-term therapeutic effects of acute inhibition of glutamate receptors should also be examined.

Abbreviations

AMPA	α-amino-3-hydroxy-5-methyl-4-isoxazolepropionate
NMDA	N-methyl-D-aspartate
WT	wild type
DPBS	Dulbecco's phosphate-buffered saline
TBS	Tris buffered saline
S1BF	somatosensory barrelfield cortex
GFAP	glial fibrillary acidic protein

Acknowledgments

This work was supported by the Luke and Rachel Batten Foundation, Beat Batten Foundation and the National Institutes of Health (NIH) grants R01 NS044310 and R21 TW008433.

References

- Bible E, Gupta P, Hofmann SL, Cooper JD. Regional and cellular neuropathology in the palmitoyl protein thioesterase-1 null mutant mouse model of infantile neuronal ceroid lipofuscinosis. *Neurobiol Dis.* 2004; 16:346–359. [PubMed: 15193291]
- Bleakman D, Alt A, Nisenbaum ES. Glutamate receptors and pain. *Semin Cell Dev Biol.* 2006; 17:592–604. [PubMed: 17110139]
- Chase TN, Bibbiani F, Oh JD. Striatal glutamatergic mechanisms and extrapyramidal movement disorders. *Neurotox Res.* 2003; 5:139–146. [PubMed: 12832228]
- Consortium TIBD. Isolation of a novel gene underlying Batten disease, CLN3. *Cell.* 1995; 82:949–957. [PubMed: 7553855]
- Cooper JD. Progress towards understanding the neurobiology of Batten disease or neuronal ceroid lipofuscinosis. *Curr Opin Neurol.* 2003; 16:121–128. [PubMed: 12644737]
- Danton GH, Dietrich WD. Inflammatory mechanisms after ischemia and stroke. *J Neuropathol Exp Neurol.* 2003; 62:127–136. [PubMed: 12578222]
- Engblom D, Bilbao A, Sanchis-Segura C, Dahan L, Perreau-Lenz S, Balland B, Parkitna JR, Lujan R, Halbout B, Mameli M, Parlato R, Sprengel R, Luscher C, Schutz G, Spanagel R. Glutamate receptors on dopamine neurons control the persistence of cocaine seeking. *Neuron.* 2008; 59:497–508. [PubMed: 18701074]
- Fan MM, Raymond LA. N-methyl-D-aspartate (NMDA) receptor function and excitotoxicity in Huntington's disease. *Prog Neurobiol.* 2007; 81:272–293. [PubMed: 17188796]
- Farfara D, Lifshitz V, Frenkel D. Neuroprotective and neurotoxic properties of glial cells in the pathogenesis of Alzheimer's disease. *J Cell Mol Med.* 2008; 12:762–780. [PubMed: 18363841]
- Gigler G, Moricz K, Agoston M, Simo A, Albert M, Benedek A, Kapus G, Kertesz S, Vegh M, Barkoczy J, Marko B, Szabo G, Matucz E, Gacsalyi I, Levay G, Harsing LG Jr, Szenasi G. Neuroprotective and anticonvulsant effects of EGIS-8332, a non-competitive AMPA receptor antagonist, in a range of animal models. *Br J Pharmacol.* 2007; 152:151–160. [PubMed: 17603549]
- Goebel HH. The neuronal ceroid-lipofuscinoses. *J Child Neurol.* 1995; 10:424–437. [PubMed: 8576551]
- Goebel HH, Wisniewski KE. Current state of clinical and morphological features in human NCL. *Brain Pathol.* 2004; 14:61–69. [PubMed: 14997938]
- Graham RK, Pouladi MA, Joshi P, Lu G, Deng Y, Wu NP, Figueroa BE, Metzler M, Andre VM, Slow EJ, Raymond L, Friedlander R, Levine MS, Leavitt BR, Hayden MR. Differential susceptibility to excitotoxic stress in YAC128 mouse models of Huntington disease between initiation and progression of disease. *J Neurosci.* 2009; 29:2193–2204. [PubMed: 19228972]
- Greene IP, Lee EY, Prow N, Ngwang B, Griffin DE. Protection from fatal viral encephalomyelitis: AMPA receptor antagonists have a direct effect on the inflammatory response to infection. *Proc Natl Acad Sci U S A.* 2008; 105:3575–3580. [PubMed: 18296635]
- Gressens P, Spedding M, Gigler G, Kertesz S, Villa P, Medja F, Williamson T, Kapus G, Levay G, Szenasi G, Barkoczy J, Harsing LG Jr. The effects of AMPA receptor antagonists in models of stroke and neurodegeneration. *Eur J Pharmacol.* 2005; 519:58–67. [PubMed: 16112106]
- Gundersen HJ, Jensen EB. The efficiency of systematic sampling in stereology and its prediction. *J Microsc.* 1987; 147:229–263. [PubMed: 3430576]
- Karl T, Pabst R, von Horsten S. Behavioral phenotyping of mice in pharmacological and toxicological research. *Exp Toxicol Pathol.* 2003; 55:69–83. [PubMed: 12940631]
- Kielar C, Maddox L, Bible E, Pontikis CC, Macauley SL, Griffey MA, Wong M, Sands MS, Cooper JD. Successive neuron loss in the thalamus and cortex in a mouse model of infantile neuronal ceroid lipofuscinosis. *Neurobiol Dis.* 2007; 25:150–162. [PubMed: 17046272]
- Kovacs AD, Pearce DA. Attenuation of AMPA receptor activity improves motor skills in a mouse model of juvenile Batten disease. *Exp Neurol.* 2008; 209:288–291. [PubMed: 17963751]
- Kovacs AD, Weimer JM, Pearce DA. Selectively increased sensitivity of cerebellar granule cells to AMPA receptor-mediated excitotoxicity in a mouse model of Batten disease. *Neurobiol Dis.* 2006; 22:575–585. [PubMed: 16483786]

- Lane DA, Lessard AA, Chan J, Colago EE, Zhou Y, Schlussman SD, Kreek MJ, Pickel VM. Region-specific changes in the subcellular distribution of AMPA receptor GluR1 subunit in the rat ventral tegmental area after acute or chronic morphine administration. *J Neurosci*. 2008; 28:9670–9681. [PubMed: 18815253]
- Manahan-Vaughan D, von Haebler D, Winter C, Juckel G, Heinemann U. A single application of MK801 causes symptoms of acute psychosis, deficits in spatial memory, and impairment of synaptic plasticity in rats. *Hippocampus*. 2008; 18:125–134. [PubMed: 17924525]
- Matucz E, Moricz K, Gigler G, Simo A, Barkoczy J, Levay G, Harsing LG Jr, Szenasi G. Reduction of cerebral infarct size by non-competitive AMPA antagonists in rats subjected to permanent and transient focal ischemia. *Brain Res*. 2004; 1019:210–216. [PubMed: 15306255]
- Mitchison HM, Bernard DJ, Greene ND, Cooper JD, Junaid MA, Pullarkat RK, de Vos N, Breuning MH, Owens JW, Mobley WC, Gardiner RM, Lake BD, Taschner PE, Nussbaum RL. Targeted disruption of the *Cln3* gene provides a mouse model for Batten disease. *The Batten Mouse Model Consortium* [corrected]. *Neurobiol Dis*. 1999; 6:321–334. [PubMed: 10527801]
- Paxinos, G.; Franklin, KBJ. *The mouse brain in stereotaxic coordinates*. San Diego: Academic Press; 2001.
- Pears MR, Cooper JD, Mitchison HM, Mortishire-Smith RJ, Pearce DA, Griffin JL. High resolution 1H NMR-based metabolomics indicates a neurotransmitter cycling deficit in cerebral tissue from a mouse model of Batten disease. *J Biol Chem*. 2005; 280:42508–42514. [PubMed: 16239221]
- Phillips SN, Benedict JW, Weimer JM, Pearce DA. CLN3, the protein associated with batten disease: structure, function and localization. *J Neurosci Res*. 2005; 79:573–583. [PubMed: 15657902]
- Pontikis CC, Cella CV, Parihar N, Lim MJ, Chakrabarti S, Mitchison HM, Mobley WC, Rezaie P, Pearce DA, Cooper JD. Late onset neurodegeneration in the *Cln3*^{-/-} mouse model of juvenile neuronal ceroid lipofuscinosis is preceded by low level glial activation. *Brain Res*. 2004; 1023:231–242. [PubMed: 15374749]
- Rider JA, Rider DL. Batten disease, a twenty-eight-year struggle: past, present and future. *Neuropediatrics*. 1997; 28:4–5. [PubMed: 9151308]
- Venneti S, Wiley CA, Kofler J. Imaging microglial activation during neuroinflammation and Alzheimer's disease. *J Neuroimmune Pharmacol*. 2009; 4:227–243. [PubMed: 19052878]
- Weimer JM, Benedict JW, Getty AL, Pontikis CC, Lim MJ, Cooper JD, Pearce DA. Cerebellar defects in a mouse model of juvenile neuronal ceroid lipofuscinosis. *Brain Res*. 2009; 1266:93–107. [PubMed: 19230832]
- Weimer JM, Custer AW, Benedict JW, Alexander NA, Kingsley E, Federoff HJ, Cooper JD, Pearce DA. Visual deficits in a mouse model of Batten disease are the result of optic nerve degeneration and loss of dorsal lateral geniculate thalamic neurons. *Neurobiol Dis*. 2006; 22:284–293. [PubMed: 16412658]
- Wohrl R, Eisenach S, Manahan-Vaughan D, Heinemann U, von Haebler D. Acute and long-term effects of MK-801 on direct cortical input evoked homosynaptic and heterosynaptic plasticity in the CA1 region of the female rat. *European Journal of Neuroscience*. 2007; 26:2873–2883. [PubMed: 18001284]

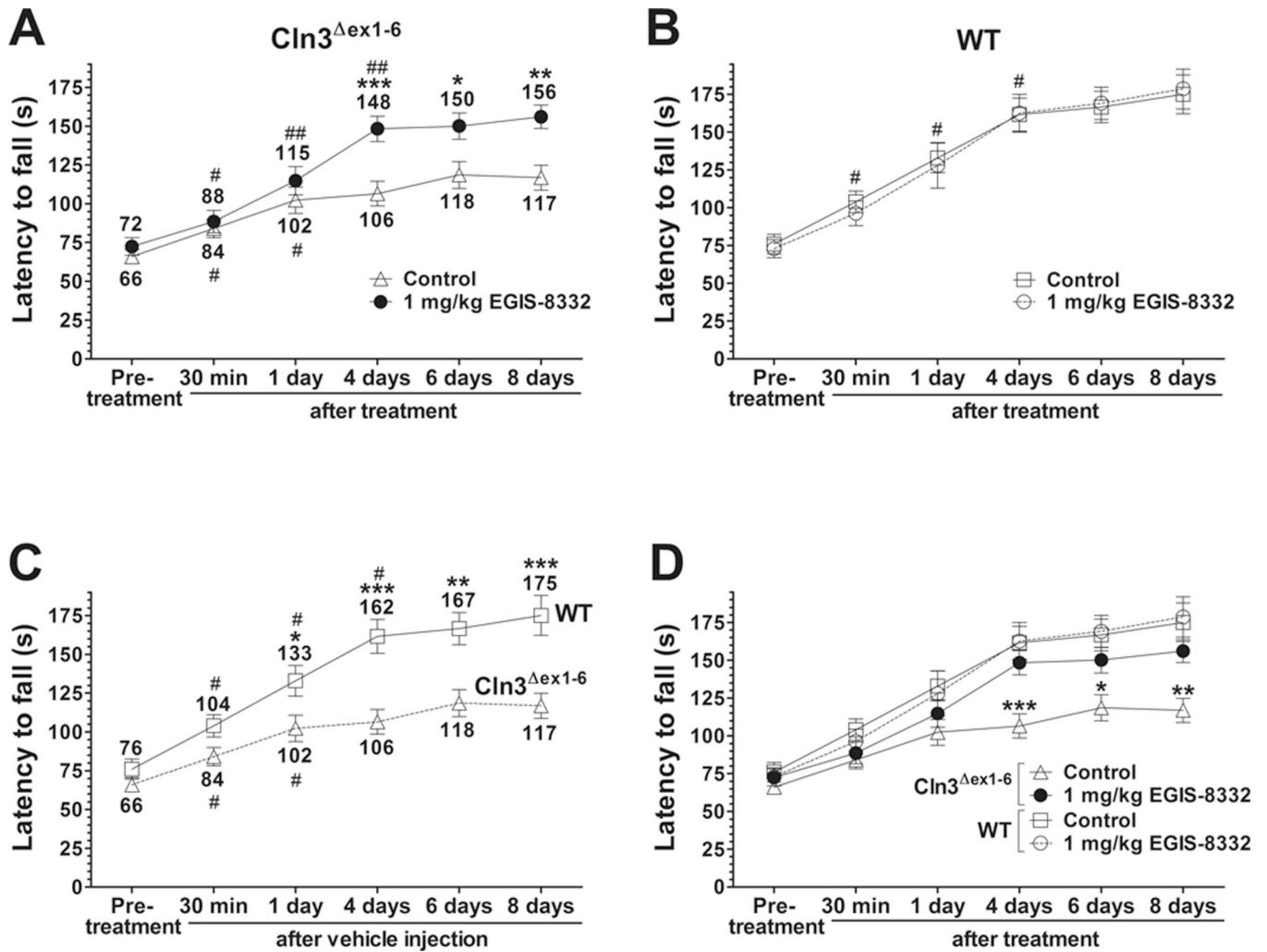


Fig. 1. A single intraperitoneal injection of the non-competitive AMPA receptor antagonist, EGIS-8332, induces a delayed but prolonged improvement of motor skills in 6-7-month-old *Cln3*^{Δex1-6} mice

An accelerating rotarod (from 0 to 24 rpm in 240 s) was used to measure the motor skills of 6-7-month-old *Cln3*^{Δex1-6} and wild type (WT) mice. Mice were intraperitoneally injected with either the non-competitive AMPA antagonist, EGIS-8332 (1 mg/kg) or the vehicle of the drug (Control). Data points represent mean \pm S.E.M. of the time (s) mice were able to stay on the rotating rod. Repeated measures two-way ANOVA was applied to compare Control and EGIS-8332-treated *Cln3*^{Δex1-6} mice (* $p < 0.05$, ** $p < 0.01$ and *** $p < 0.001$) as well as Control WT and *Cln3*^{Δex1-6} mice. Repeated measures one-way ANOVA was used to compare the motor performances between two consecutive time points (# $p < 0.05$, ## $p < 0.01$). (A) EGIS-8332 induces a delayed but prolonged improvement of motor skills in 6-7-month-old *Cln3*^{Δex1-6} mice ($n=15$). *: Control vs. EGIS-8332; #: comparison between two consecutive time points. (B) EGIS-8332 does not affect the motor skills of 6-7-month-old WT mice ($n=12-13$). #: comparison between two consecutive time points. (C) Control, vehicle-injected *Cln3*^{Δex1-6} mice ($n=15$), differently from WT mice ($n=13$), had only a limited ability to improve their motor skills during the repeated rotarod test trials. *: WT vs. *Cln3*^{Δex1-6}; #: comparison between two consecutive time points. (D) Four days after the injection of EGIS-8332, *Cln3*^{Δex1-6} mice reached the the same motor skill

level as their WT counterparts and stayed at the WT skill level even four days later (*: WT vs. *Cln3^{Δex1-6}*).

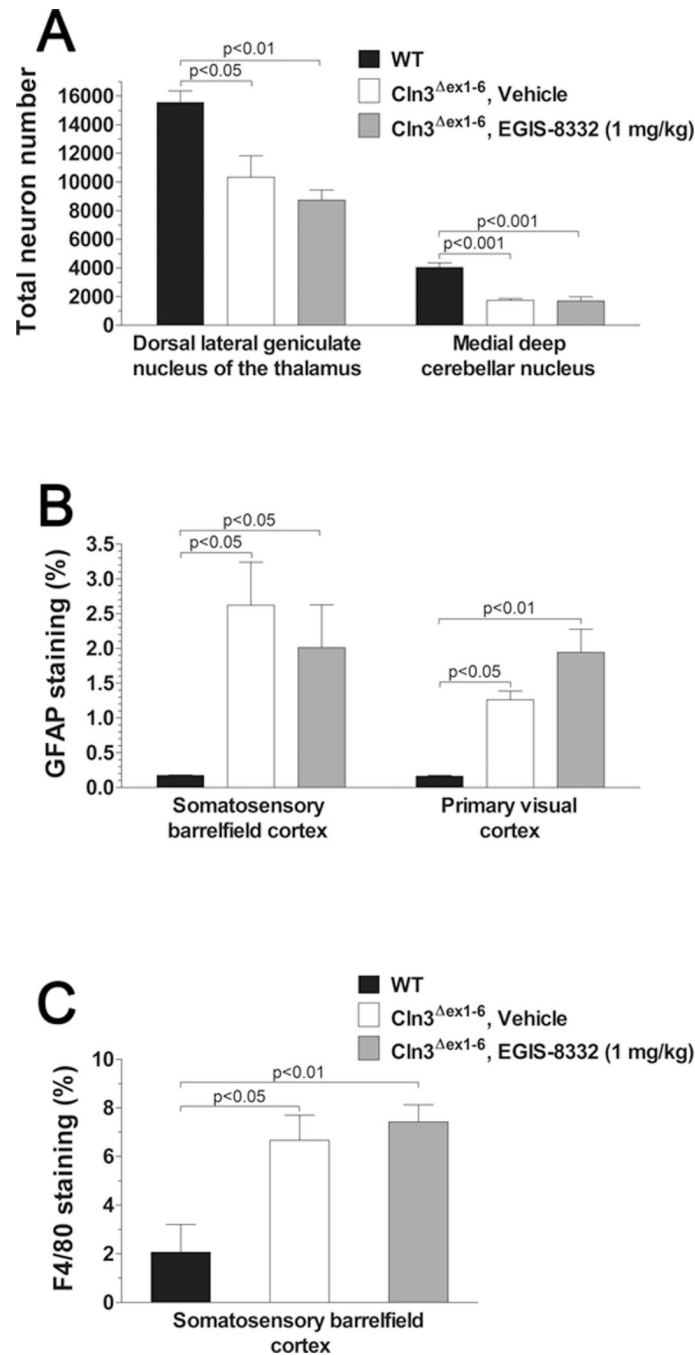


Fig. 2. A single intraperitoneal injection of the non-competitive AMPA receptor antagonist, EGIS-8332, has no effect on the previously described neuropathological changes in 7-month-old *Cln3*^{Δex1-6} mice

Four 7-month-old wild type (WT) mice were perfusion-fixed and their brains were histologically analyzed. Four vehicle-injected and four EGIS-8332-treated 7-month-old *Cln3*^{Δex1-6} mice were perfusion-fixed eight days after the treatment, and their brains were also histologically analyzed. Columns and bars represent mean \pm S.E.M. **(A) EGIS-8332 has no effect on the selective neuron loss in the thalamus and cerebellum.** Unbiased stereological estimates of the number of large projection neurons in the dorsal lateral geniculate nucleus of the thalamus and in the medial deep cerebellar nucleus. **(B)**

EGIS-8332 does not affect astrocytic activation in the cortex. Quantitative determination of astrocytosis in the somatosensory barrelfield cortex and the primary visual cortex was performed by thresholding image analysis following immunohistochemical staining for the astrocytic marker, GFAP. **(C) EGIS-8332 does not affect microgliosis in the cortex.**

Quantitative determination of microgliosis in the somatosensory barrelfield cortex was performed by thresholding image analysis following immunohistochemical staining for the microglial marker F4/80.

Statistical analysis (one-way ANOVA with Bonferroni's post-test) revealed that EGIS-8332 had no effect on the selective neuron loss, astrocytosis and microglial activation. Statistical significances between WT and *Cln3^{Δex1-6}* mice are indicated in the graphs.

Table 1

Concentrations of EGIS-8332 in the plasma and brain of 7-month-old *Cln3^{Δex1-6}* mice at different time points after a single i.p. administration (1 mg/kg); n=4 mice at each time point. EGIS-8332 levels were measured by HPLC-MS/MS.

Time after administration	Plasma, ng/ml	Brain, ng/g
15 min	837.0±116.0	81.1±12.6
1 h	233.7±18.1	41.5±9.6
3 h	21.7±5.6	3.0±1.0
8 h	1.3±0.1	ND
24 h	ND	ND
48 h	ND	ND

ND: non-detectable